Journal of Materials Chemistry B

ROYAL SOCIETY OF CHEMISTRY

PAPER

View Article Online
View Journal | View Issue

Cite this: J. Mater. Chem. B, 2025, 13, 1980

Biological activation of Fenton reaction in polymeric nanoreactors driven by ferrocene-containing membranes: a microenvironment dependent study†

Alejandro González Vivancos,[a] Yang Zhou,[a] Uwe Lappan,[a] Susanne Boye,[a] Laura Muñoz-Moreno,[b] Dietmar Appelhans *[a] and Silvia Moreno *[ab]

Nanocatalytic medicine for treating cancer requires effective, versatile and novel tools and approaches to significantly improve the therapeutic efficiency for the interactions of (non-)enzymatic reactions. However, it is necessary to develop (non-)enzymatic nanotechnologies capable of selectively killing tumour cells without harming normal cells. Their therapeutic characteristics should be the adaption of tumours' extra- and intracellular environment to being specifically active. To contribute to this common goal, we propose the use of pH- and redox-responsive ferrocene containing polymersomes (FcPsomes). This allows the regulation of their biological activities for the controlled production of radicals *via* the Fenton reaction and the transport and release of cargo molecules *via* (destroying) host–guest interactions. This is provided by the Fc-membrane composition of FcPsomes showing different pH responsive active membrane, meaning the membrane permeability is triggering the Fenton reaction. The modulation of radical production is validated by various spectroscopic techniques. Moreover, these nanocontainers allow biological action of glucose oxidase (GOx) as therapeutic enzyme to produce glucono-1,5-lactone as proton source and hydrogen peroxide, initiating the Fenton reaction, in their interior. This provides a synergistic cancer therapeutic treatment for the starvation of hydrogen peroxide, but also ROS-mediated chemodynamic therapy at defined pH values. By modulating membrane permeability, we achieve environmentally regulated and locally driven therapeutic activity in the confinement of FcPsomes, ensuring specificity and safety treatments. The versatility of this platform extends beyond their specific application, allowing for their beneficial therapeutic use, for example, in signaling pathways of cells through the integration of various enzymes in FcPsomes.

Received 8th August 2024,
Accepted 19th December 2024

DOI: 10.1039/d4tb01776e

rsc.li/materials-b

Introduction

Nanocatalytic medicine and combined strategies for cancer treatment present a promising and multifaceted approach that is gaining attention.[1–5] The key to progress lies in the establishment of multifunctional nanomaterials. It is known that these nanomaterials are capable of carrying out enzymatic reactions, either based on natural enzymes (NEs) or artificial units, such as nanozymes (NZs). NZs are understood to be nanomaterials with enzyme-like properties.[3,6,7] Both biocatalytic entities are being used in the creation of theragnostic nanoplatforms, which integrate diagnostic and therapeutic functions.[7] The development of advanced nanocatalytic approaches offers the potential for real-time imaging of tumours[8,9] and the simultaneous delivery of therapeutic agents.[2,6,7] The advantages of nanoparticles (NPs) in drug delivery are well known, especially from the point of view of stability, control and targeting. Nevertheless, the combination of these two elements with enzymatic cavities has the effect of expanding their therapeutic functions and even enhancing the effective treatments, which are initiated by several mechanisms of action.[10–14]

An example of a nanocatalytic entity for nanomedicine is ferrocene-containing nanoparticles.[15–18] The intrinsic chemical and therapeutic properties (*e.g.* stability, redox activity and biocompatibility) of ferrocene offer an attractive candidate for integration into polymeric nanoparticles designed for drug delivery and cancer treatment, providing multiple and versatile properties.[5,10,19,20] Highlighting the redox properties of ferrocene, its presence is used to make it possible to design a

[a] Leibniz Institute of Polymer Research Dresden (IPF), Dresden, Germany. E-mail: silvia.morenop@uah.es, applhans@ipfdd.de
[b] Department of Organic and Inorganic Chemistry, University of Alcalá, 28805 Madrid, Spain

† Electronic supplementary information (ESI) available. See DOI: https://doi.org/10.1039/d4tb01776e

polymeric matrix that responds to the oxidative environment. This is a typical action in cancerous tissue. Furthermore, drugs, integrated in nanocatalytic particles, can be selectively released at the tumor site, minimizing side effects on healthy tissue.[10,18] In addition, ferrocene enhances the generation of reactive oxygen species (ROS, Fenton reaction), leading to the destruction of cancer cells.[21] These species also contribute to promote the weakening of the dense extracellular matrix (ECM) and even activate matrix metalloproteinases (MMPs) that promote ECM degradation.[22] Polymeric entities with ferrocene units in their structure offer an innovative multimodal approach that can enhance any of the known treatments through synergistic or combined effects.[5,10,11,20] However, modulation of the biological activity of ferrocene units is imperative, representing a promising frontier in cancer treatment, with the potential to lead more effective and personalized therapeutic strategies.[14,16,18,21,23]

Our contribution to the field of nanocatalytic nanomedicine lies in the successful design, formation, and characterization of pH- and redox-responsive polymersomes (Psomes). These Psomes incorporate ferrocene (Fc) units within their hydrophobic membranes, creating ferrocene-containing Psomes (FcPsomes).[24] The Fc units in FcPsomes can produce the desired radicals under the conditions required for the Fenton reaction. The degree of produced radicals in the membrane of FcPsomes is regulated by the pH-dependent permeability of the FcPsomes membrane. This results in a lower production of radicals within the collapsed membrane state of FcPsomes at physiological pH, in comparison to the swollen membrane state of FcPsomes in an acidic environment. This is caused by the reduced diffusion capacity of H_2O_2 substrate to the Fc units in the collapsed membrane state. Additionally, the integration of glucose oxidase (GOx) into the FcPsomes membrane using a post-loading approach enhances the efficiency of radical production.[24] Moreover, the extensive versatility of FcPsomes is also achieved through the GOx-mediated docking and undocking process of β-cyclodextrin-modified model molecules *via* host–guest interaction, which is dependent on the redox state of Fc units within the swollen FcPsomes membrane.[13,25] It is important to note that all of these FcPsomes exceed 120 nm in size by Cryo-TEM. Achieving reproducible structures becomes challenging with even slight modifications to the composition of the ferrocene-containing block copolymers (FcBCPs). Additionally, their preparation needs the use of organic solvents, which complicates the subsequent incorporation of biological molecules and hinders clear observation of phase separation in Cryo-TEM (Fig. S12, ESI†). In this work, we aim to fine-tune the size and structural properties to develop a more versatile and adaptable nanoplatform.

Concluding the progress of our nanocatalytic compartments for their use in the field of nanocatalytic nanomedicine, the membrane of FcPsomes with and without post-loaded GOx outlines a lower pH-adaptation towards the physiological environment. This is caused by the standard use of block copolymer A (BCP A, Scheme 1) which results in the formation of a less hydrophobic membrane. In general, the pH sensitivity of Psomes membrane can be readily modulated by small changes

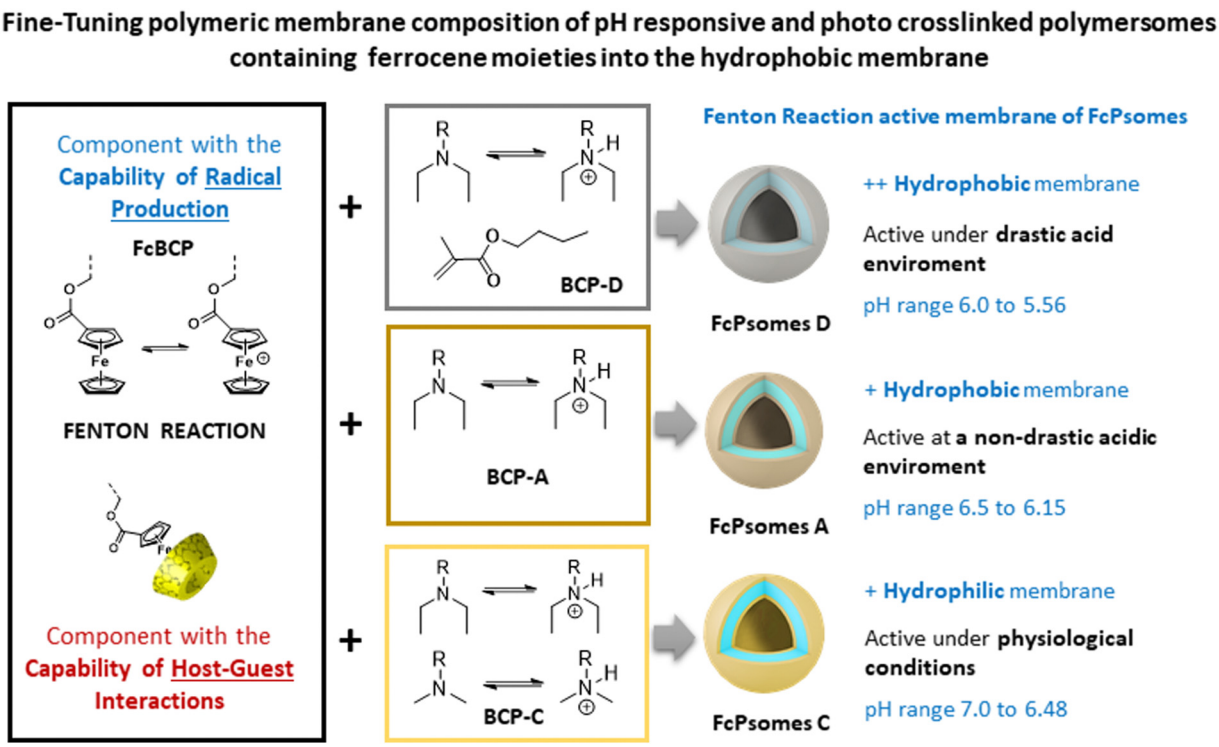

Scheme 1 Representation of different polymeric nanodevices (ferrocene-containing polymeric vesicles, FcPsomes) with the ability to regulate the ferrocene-based properties (Fenton reaction or/and host–guest interactions) under different pH therapeutic windows. Membranes of FcPsomes A, C and D with different hydrophobic balance and permeability are obtained by mixing different block copolymers.

in the BCP composition. These Psomes are implemented with even more hydrophobic membranes.[7,10] Consequently, it is possible to design pH-dependent active or permeable nanocompartments at selected pH values.[23,26,27] This adaptive pH characteristic is essential for the further development of FcPsomes membrane for its potential use in the intra- and extracellular matrix of tumour tissues. Moreover, FcPsomes[24,25] represent a limited incorporation of biomacromolecules into the lumen due to the use of organic solvent for their formation. To enhance the potential of FcPsomes, it is essential to optimise the preparation process to facilitate the incorporation of biomacromolecules inside the lumen (free organic solvent protocol). Moreover, there is a need for the development of stable FcPsomes membranes with varying hydrophilic/hydrophobic balances.

The motivation of this work is to generate therapeutic nanoreactors for nanocatalytic nanomedicine, where the properties of NEs (GOx, to continuously produce H_2O_2) and NZs (ferrocene units in the membrane, to generate hydroxyl radicals ($^{\bullet}OH$)) are combined to enhance the Fenton reaction (Scheme 1, Chemodynamic Therapy, CDT). Moreover, the nanoreactors used due to their pH-sensitivity, a local acidification promotes CDT and a possible intracellular cargo release.[15,16] The generated hydroxyl radicals are highly reactive and have a very short lifetime, leading to limited diffusion distance and rapid recombination. To overcome the potentially reduced therapeutic efficiency, GOx plays a critical role within the lumen of FcPsomes by continuously supplying the Fc units in the membrane with the required substrate, H_2O_2, through the oxidative conversion of glucose to gluconic acid and H_2O_2. This is achieved through by the oxidative conversion of glucose to gluconic acid and H_2O_2. In addition, the therapeutic nanoreactors should exert their maximal cytotoxic effect in the tumour environments. This requires the development of FcPsomes with a more hydrophobic membrane, which should provide an essential therapeutic window for the Fenton reaction to more acidic conditions (pH 5.5–6.0). This approach to designing nanoreactors with tumour-activatable cascade-reactions represents an insightful paradigm for targeted and personalised cooperative cancer therapy.

Herein, we report several well-defined cross-linked and multi-responsive FcPsomes (Scheme 1 and Fig. 1(A)), realised by the co-assembly of two different block copolymers (BCPs),

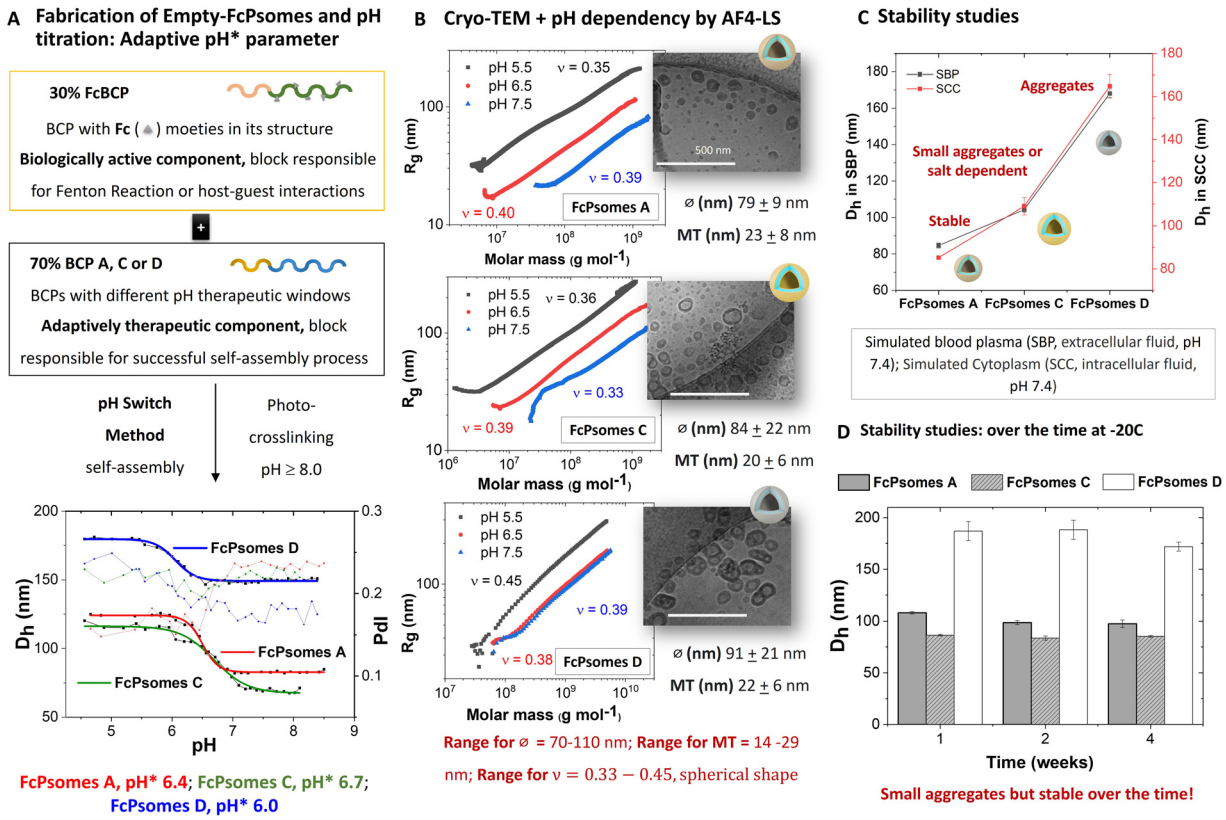

Fig. 1 (A) Representation of the fabrication of the different FcPsomes, where the composition of FcBCP (30%) is fixed and then combined with one of the other 3 BCPs (A, C or D) giving empty-FcPsomes A, C or D. pH dependent size determination in 1 mM PBS by DLS using 0.5 mg mL^{-1}. The pH* was determined by using Boltzmann fit and taking the inflexion point. The fine lines illustrate the sample's polydispersity index (<0.250). (B) pH dependent scaling parameter (ν) of empty-FcPsomes. Scaling plots, R_g (circles) *vs.* Molar masses determined by AF4-LS. Theoretical values for ν: range from 0.33 for spheres, over 0.5 to 0.7 for random coil macromolecules to 1 for rigid rods. Conditions: 0.5 mg mL^{-1} in 1 mM PBS at pH 5.5, 6.5 or 7.5. Diameter (ø) and membrane thickness (MT) of empty-FcPsomes by Cryo-TEM at pH 8. (C) Stability study and size determination of FcPsomes by DLS in simulated body fluids (SBP, SCC) after a short incubation time. D_h values in 1 mM PBS are 86, 157 and 98 nm for FcPsomes A, D and C, respectively. (D) Stability study by DLS of empty FcPsomes solutions after being frozen (−20 °C) for extended periods of time (1 mg mL^{-1} in 10 mM NaCl).

using ferrocene-containing (30 wt% of FcBCP) synthesised by the reversible addition–fragmentation chain-transfer (RAFT, Fc-BCP) polymerisation[24] and non-ferrocene-containing (70 wt%) BCPs synthesised by atom transfer radical polymerisation (ATRP, BCP-A, C and D).[23,24,27] The self-assembly behaviour and a deeper study of their physico-chemical and conformational properties are described, investigated by cryogenic transmission electron microscopy (cryo-TEM), dynamic light scattering (DLS), zeta potential and asymmetric flow-field flow fractionation coupled to light scattering (AF4-LS). Moreover, optimised electron paramagnetic resonance (EPR) spectroscopy measurements and enzymatic assays based on fluorescence measurements were used to demonstrate the potential regulation of H_2O_2 consumption or radical production of several FcPsomes under different microenvironments,[28] also achieving the required therapeutic window at pH 6. Finally, GOx-loaded FcPsomes demonstrate their potential in toxicity assay, how the GOx enzyme enhances the production of radicals and consequently the essential toxicity to reduce cell viability, in comparison to pure FcPsomes.

Results and discussion

Synthesis and characterization of ferrocene-containing polymeric vesicles

For the formation of FcPsomes A, C and D (Scheme 1) three different pH responsive and crosslinkable BCPs (BCP-A, BCP-C, BCP-D) have been synthesised.[23,26,27] These BCPs are defined as interchangeable adaptively therapeutic components. The synthesised ferrocene-containing, pH responsive and crosslinkable block copolymer (FcBCP) is defined as fixed therapeutic component (Fig. 1(A)).[24] All of them feature poly(ethylene glycol) (PEG) as a hydrophilic segment and 3,4-dimethylmaleic imidobutyl methacrylate (DMIBMA) as a crosslinker in the hydrophobic block. However, the composition of their hydrophobic segments varies with the intention of providing a membrane permeability of different nature, which will ultimately influence the capacity to host biomacromolecules and other cargo molecules in their membrane. BCP-A and FcBCP have just one kind of pH responsive monomer, 2-(*N*,*N*′-diethylamino)ethyl methacrylate (DEAEMA, pK_B 5.2) for tuning the membrane permeability of FcPsomes A. BCP-D exhibits a greater hydrophobicity as a result of the defined replacement of DEAEMA with *n*-butyl methacrylate. In comparison to BCP-A, BCP-C exhibits a greater hydrophilic character. This is attributed to the partial substitution of DEAEMA by DMAEMA (2-(*N*,*N*′-dimethylamino)ethyl methacrylate, pK_B 5.7), implying protonation at a higher pH, that is, a membrane permeability closer to physiological pH.[26,27] The BCPs were analysed by SEC-MALS to determine their molar masses and dispersity (*Đ*) values, supplementing the calculated molar masses by ^{1}H-NMR spectroscopy. The calculation of the molecular composition is shown in Fig. S2 and Table S1 (ESI†). Further detailed synthesis (Table S2, ESI†) and characterisation are shown in the ESI.†

One of the main achievements of this work has been to optimize the preparation of FcPsomes, particularly regarding to the avoidance of organic solvents, which permits the incorporation of bio(macro)molecules within the vesicles without compromising their stability. The efficiency of different ratios of BCPs/FcBCP was validated without compromising vesicle formation and reproducibility, while maintaining a high content of Fc. Non-ferrocene-containing BCPs facilitate vesicle formation due to their closer alignment to the theoretical block ratio (1 : 2) between hydrophilic and hydrophobic components.[28,29] Finally, the use of BCPs with slight changes in their hydrophobic block enables the formation of FcPsomes thereby broadening their biological applications. The self-assembly of different mixtures of BCPs (70 wt% BCP-X/30 wt% FcBCP; X = A, C or D) to form empty-FcPsomes was based on the well-established pH switch method and the subsequent photocrosslinking process by UV lamp.[23,26,27] The use of higher wt% of FcBCP in assembled FcPsomes resulted in less stable vesicles and were not further investigated (Fig. S3–S6, ESI†). Thus, it was decided to stick with 30 wt% (Fig. S3–S5 and Table S4, ESI†).

The reproducibility of the size changes due to the swelling and deswelling of the empty-FcPsomes (A, C and D in 10 mM NaCl) by pH switch cycles was measured by DLS. The results demonstrate that FcPsomes remain stable for at least five cycles of swelling and deswelling (Fig. S3–S5, ESI†). Although stability is a prerequisite, the key parameter is pH* which defines the semi-open state of the vesicles (Fig. 1(A)). pH* values are generally dependent on the salt and BCP composition.[26,27] To apply and trigger the Fenton reaction within defined pH windows, it is important to ascertain the starting point of swelling and the fully swollen state of FcPsomes A, C and D (Fig. 1(A) and Table S6, ESI†). First, pH* values of 6.0, 6.4 and 6.7 were determined for FcPsomes D, A and C, respectively. It can be observed that as the hydrophobicity of BCP decreases (D > A > C), the pH* increases. The transition curve from the starting point of swelling to the swollen state for FcPsomes C is a very gradual change (extended state of permeability), with a range from 7.25 (start of opening) to 6 (fully swollen) pH values. In contrast, for FcPsomes A, the change is much sharper (soft but rapid shift towards an acidic environment) with a range from 6.75 to 6.25 pH values. The most notable difference is observed in the case of FcPsomes D, where the opening process starts at pH 6.25 and achieves pH 5.5 for the complete state of opening (a drastic shift towards an acidic environment).

The morphology (vesicular structure), diameter and membrane thickness were confirmed by cryo-TEM (Fig. 1(B)). The resulting mean diameters ($\varnothing$) for FcPsomes ($\varnothing_{FcA}$ 79 ± 9 nm; $\varnothing_{FcC}$ 84 ± 22 nm; $\varnothing_{FcD}$ 91 ± 21 nm) and membrane thickness (MT) (MT ≈ around 20 nm in all cases) are in the range of previously published results.[23,27,30] Although larger hydrodynamic diameters for FcPsomes D are observed by DLS, cryo-TEM results show that the diameter is not drastically different than for FcPsomes A and C. This can be attributed to small aggregates. Based on these results, we conclude that the membrane permeability can be adjusted without significantly affecting the size of the nanocontainers—an aspect that is crucial for loading efficiency, particularly with bulky cargoes

like enzymes. Additionally, we demonstrate that employing an organic solvent-free protocol yields similar structures without phase separation, as seen in the case of pure FcPsomes (Fig. S12, ESI†). Zeta potential measurements were carried out using empty-FcPsomes at pH 9 (collapsed state, CS) and at pH 5 (swollen state, SS) in 10 mM NaCl and in 1 mM PBS (Table S5, ESI†). In all cases, the surface charge values increase when transitioning from the collapsed state to the swollen state. It can be observed that FcPsomes D give higher values than the other two FcPsomes (1 mM PBS): FcPsomes A: +18.1 (SS), −1.2 (CS) mV; (FcPsomes C: +16.0 (SS)), +1.6 (CS) mV; (FcPsomes D: +28.3 (SS), −3.1 (CS) mV). An increase in the zeta potential value of a nanoparticle generally implies a higher stability of the colloidal suspension. It may be that the formation of small aggregates, confirmed from the outset of DLS, implies a higher electrostatic repulsion and stabilises the colloidal suspension.

To obtain more depth information about stability in environments closer to biological ones, simulated biological fluids were used, as a valuable tool to better understand the solution state of FcPsomes in more complex environments (simulated blood plasma (SBP) and simulated cytoplasm (SCC)). Thus, the D_h results of the FcPsomes after short term incubation (Fig. 1(C)) indicate that the difference between SBP and SCC fluids is negligible. Furthermore, the differences in their stability behaviour in comparison with 1 mM PBS are also insignificant for all FcPsomes systems. Colloidal stability after storage for different periods was further studied by DLS, showing stability after 4 weeks at −20 °C (Fig. 1(D)).

To complete the structural characterization and pH dependency of the different FcPsomes, AF4-LS was carried out (Fig. 1(B) and Fig. S1, Table S3, Fig. S8, ESI†). AF4-LS as a separation method overcomes the limitations of other techniques, for example the lack of a stationary phase minimises the tendency for sample adsorption and degradation. This results in a gentle separation and ensures the intact structure of the loaded Psomes during the measurements as previously shown.[23,24,27,31] The molar masses and size distributions of the different samples were determined in 1 mM PBS at different pH values. The conformation plot (radius of gyration (R_g) *versus* M_w) gives valuable information about the compactness and molecular shape of FcPsomes by using the scaling parameter (ν, slope of the plot, details in (ESI†), Fig. 1(B)). FcPsomes possess a scaling exponent in the range of 0.33–0.38 at pH 7.5, which is close to the theoretical value of hard sphere object (0.33). At lower pH values, such as 6.5 and 5.5, the ν values change slightly, but they are all in the range of spherical objects, proving that despite the swelling and having two types of BCP (FcBCP/BCP-X: X = A, C or D) in the same vesicle, the structure is maintained. But an important point to note is that in the case of FcPsomes D, once more, at pH 6.5 it is collapsed, and a more drastic pH environment is needed to observe its swelling. The low pH also leads to more irregular structures observed in cryo-TEM, too. It seems likely that no defined swelling behaviour of FcPsomes D can be observed in the aggregated state at pH 6.5. This is consistent with the DLS data for the determination of starting point of swelling, pH* and fully swollen state of FcPsomes D (Fig. 1(A)). The presence of the hydrophobic Fc and *n*-butyl units in the membrane of FcPsomes D (Scheme 1) suppresses potential protonation of the DEAEMA units at pH 6.5. This (postulated) behaviour of the non-protonated membrane of FcPsomes D at pH 6.5 is also confirmed by the constant apparent density and the stable radii, only at pH 5.5 changes due to swelling can be observed (Fig. S8, ESI†). In the case of FcPsomes A and C, the apparent density decreases as expected with decreasing pH, while the radii increase. The swelling behaviour of FcPsomes A and C is more dominated by the pH-responsive tertiary amino groups within the FcPsomes membrane and can better counterbalance the hydrophobicity of the membrane-integrated ferrocene units in both FcPsomes (Scheme 1).

Fenton reaction regulation by EPR measurements

The amount of radicals produced in the membrane of FcPsomes is regulated by the pH-dependent membrane permeability. This results in a lower production of radicals in the collapsed membrane state of FcPsomes at physiological pH, compared to the swollen membrane state of FcPsomes in an acidic environment. The goal is to demonstrate the influence of the BCP composition in vesicular structures on radical production through EPR spectroscopy. This approach demonstrates that a more hydrophobic membrane, as observed in FcPsomes D, results in the reduction in radical generation and requires more drastic pH conditions. 5,5-Dimethyl-1-pyrroline N-oxide (DMPO) was used as a spin trap to detect and characterise the formation of free hydroxyl radicals (•OH) during the Fenton reaction to form a DMPO–OH adduct. Spin trapping is a technique whereby transient free radicals are stabilised by reacting with a spin trap to form a more stable radical adduct, which can then be analysed by EPR. It is used in biological and chemical research, offering significant insights into the mechanisms of oxidative processes.

First, it was investigated whether the concentration present in FcPsomes was sufficient to generate a detectable level of radicals measured by EPR. Fig. 2(A) shows the pattern of a characteristic EPR signal of the DMPO adduct formed by trapping the OH radical by using FcPsomes A at different pH values (from pH 5 to pH 7.5). Secondly, following the optimisation of the EPR conditions, the pH dependence of non-self-assembled FcBCP was studied. Its radical production is a pH dependent process, predominantly as a consequence of a solubility issue. At pH values above 6.5, the protonation of DEAEMA is insufficient to maintain the solubility of FcBCP, leading to a deficiency radical production (Fig. S7C and D, ESI†). The same trend is observed using FcPsomes A (Fig. 2(B)), however, the reproducibility of the measurements at permeable pH is lower, which may be influenced by the diffusion of the substrates and products, which is not the case when studying FcBCP alone. Finally, the three types of FcPsomes were evaluated (Fig. 2(C)), and it can be observed that in the case of FcPsomes D, a pH value of 5.5 is required to observing radical production. This indicates a reduction in the concentration of Fc in FcPsomes D, which is associated with a decrease in the

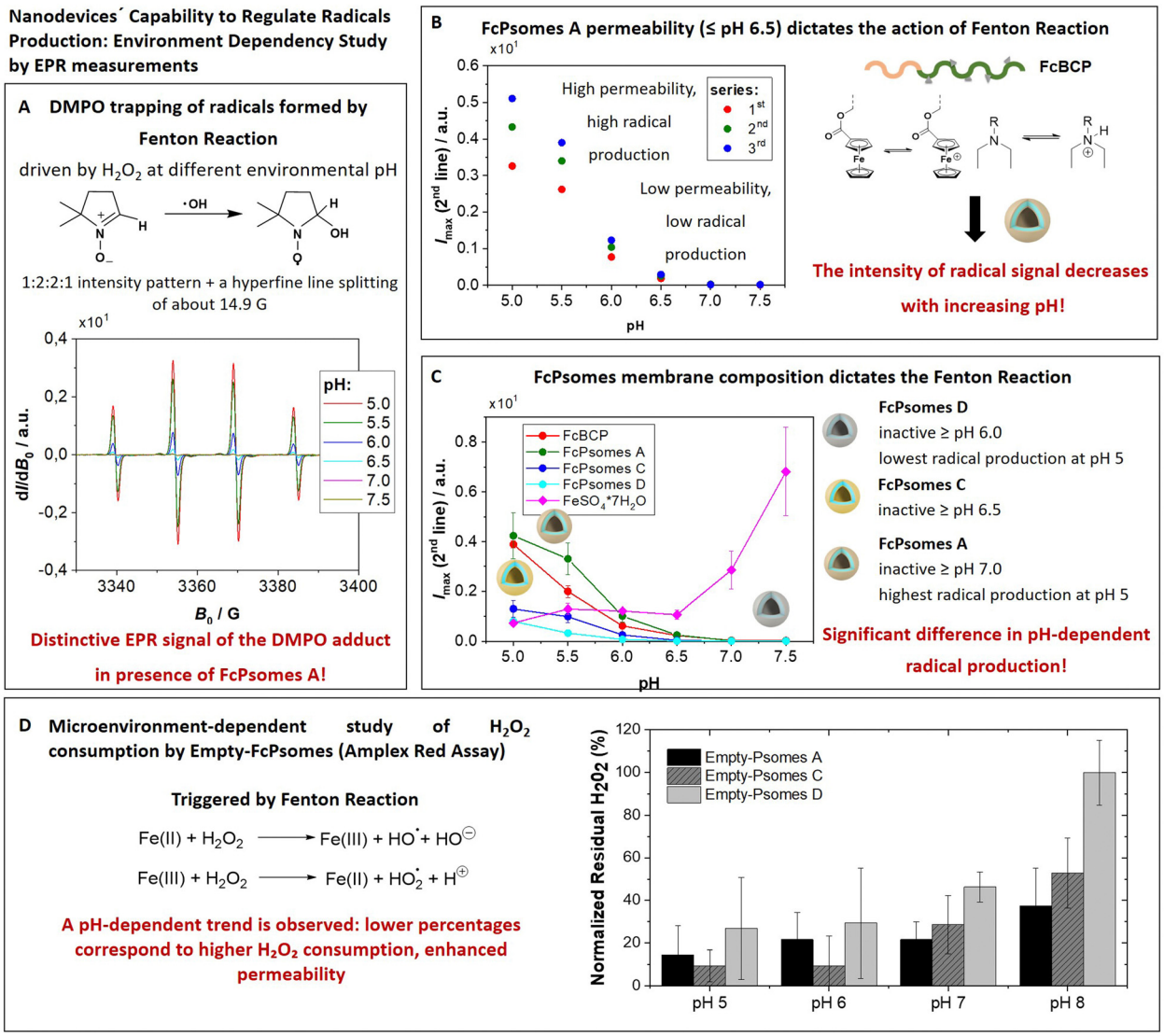

Fig. 2 Trapping of radicals at different pH with DMPO formed by the Fenton reaction of FcPsomes in the presence of hydrogen peroxide as a proof of concept. (A) The 1 : 2 : 2 : 1 intensity pattern and a hyperfine line splitting of about 14.9 G is characteristic for the DMPO adduct formed by trapping the OH radical from the Fenton reaction by using FcPsomes A at different pH values. (B) Three replicates taking the maximum intensity of second line of the signal of spin adduct for mixtures of FcBCP A, H_2O_2 and DMPO at different pH values: (C) the maximum intensity of the second line for spin-trapping experiments with FcBCP, FcPsomes A, C or D. Fe content determined by ICP-OES in 1 mg mL^{-1} solution of FcPsomes: 9.8 of Fe μg mL^{-1} in FcPsomes A, 12.4 of Fe μg mL^{-1} in FcPsomes C and 3.3 of Fe μg mL^{-1} in FcPsomes D. Conditions in all samples: 0.21 mM of ferrocene containing in 10 mM NaCl at different pH values. (D) Microenvironment-dependent study of hydrogen peroxide consumption by FcPsomes using Amplex Red assay (fluorometric measurements). It is an indirect method: the lower the fluorescence of resorufin, obtained from converted Amplex Red by myoglobin, the more active the FcPsomes are.

production of radicals. The observed decrease in Fc content in FcPsomes D can be attributed to the loss of Fc during the formation of FcPsomes D, which is a consequence of the formation of larger aggregates. For this purpose, the Fe concentration in all systems was measured by inductively coupled plasma-optical emission spectrometer (ICP-OES, Fig. 2 caption). The Fe content of FcPsomes A (9.8 μg mL^{-1}) and FcPsomes C (12.3 μg mL^{-1}) is closer than to FcPsomes D (3.3 μg mL^{-1}). Based on these data, FcPsomes A appears to be the most versatile system for a wider therapeutic window. Conversely, FcPsomes D may be more suitable for systems where a more controlled and active system may be needed, particularly in more drastic acidic environments. The pH dependence exhibits inverse relationship with the trend to $FeSO_4 \times 7H_2O$, thus demonstrating the importance of the solubility or aggregation state provided by the modified polymer or the manufactured vesicles. Nevertheless, our proof-of-concept outlines the requested functions, demonstrating the efficacy of hydrogen peroxide consumption and radical production.

Monitoring H_2O_2 consumption by empty FcPsomes in pH-dependent microenvironments

The elimination of hydrogen peroxide is preferentially understood as an antioxidant effect triggered by the FcPsomes.

Its consumption produces radicals within the vesicular structures, making them ideal systems for pumping out radicals at a given damaged site.[11,24] However, the oxidation of the Fc units by the presence of H_2O_2 also promotes the breakdown of host–guest interactions.[25]

The tracking of hydrogen peroxide consumption under different conditions (biological-like microenvironments) was the next achievement. For this, the FcPsomes (A, C and D) are incubated in different media (1 mM PBS at pH 5, 6, 7, and 8), and the hydrogen peroxide consumption is measured indirectly using the Amplex Red assay (Fig. 2(D)). It refers to the quantified concentration of residual hydrogen peroxide, for example, through the determination of higher fluorescence intensity. This implies less active or less permeable FcPsomes at which H_2O_2 cannot be decomposed by Fc units integrated in FcPsomes membrane.

This study highlights the influence of pH and salt concentration across all cases examined. The varying amounts of Fc units and the role of diffusion processes make direct comparisons of system efficiency difficult. Nonetheless, a clear pH dependency is evident, with a particularly notable difference observed in the case of FcPsomes D. The availability of such data is valuable, as it demonstrates that radical generation or potential cargo release can be modulated within specific cellular environments. However, due to variability in the data, even after multiple repetitions of the experiment, these findings should be considered indicative rather than conclusive.

Exploring the potential therapeutic enhancement of Fc units *via* continuous hydrogen peroxide supply: GOx-FcPsomes

Finally, this work aims to conduct cascade reactions that can enhance conventional therapies. As mentioned above, the hydrogen peroxide concentration could be a limiting factor due to low concentration in cells for radical production (Fenton reaction) or for oxidation reaction (release by disruption host–guest interaction). In this study, we propose a nanoplatform designed to continuously generate hydrogen peroxide in a local environment, which becomes predominantly active within an anti-tumour environment. The background for our approach differs from previous Fc-containing drug delivery systems.[32–35] Key point of them is that the disassembly and degradation of ferrocene-containing polymeric particles is a prerequisite to being successful in the establishment of nanocatalytic medicine using NZs combined with the release of drugs in the treatment of diseases.[32–35] Other option is the simultaneous hydrolytic cleavage of Fc within cancerous cells to induce ferroptosis (apoptosis of cancer cells).[33,36]

Our concept aims for long-term use by introducing pH- and salt-sensitive stable nanosystems with adaptive properties that remain intact without disassembly, exhibiting NZ characteristics. These mechanisms can be targeted within the nanocontainer framework to achieve continuous long-term regulation or activity for future intra- and extracellular matrix applications.

GOx enzyme was used as an enhancer component in FcPsomes D to supply hydrogen peroxide over an extended period after their validated anti-tumor activity of pure FcPsomes towards cancerous PC3 cell line. Due to its large size, and the combination of different BCPs, *in situ* conditions were optimised, finally using 0.01 mg mL^{-1} of GOx during the formation of the FcPsomes D (Fig. 3(B)). No predominant differences in the diameter and pH* of GOx-FcPsomes are observed compared to the empty system, determined by DLS (Fig. 3(B)). FITC-GOx was also loaded into FcPsomes D, but there were unwanted interactions that prevented it from being properly purified and therefore the loading efficiency could not be estimated (Fig. S9, ESI†). Colloidal stability was measured by DLS after three months storage at −20 °C while maintaining acceptable similar size and PDI (Table S7, ESI†). Additionally, the enzymatic activity of GOx-FcPsomes D was evaluated in comparison to FcPsomes D in presence of naked GOx, showing good retained enzymatic capacity (Fig. S13, ESI†). However, distinguishing between the swollen and collapsed states is challenging. In the swollen state, while more hydrogen peroxide is produced, its consumption also increases due to the enhanced availability of ferrocene units.

On the one hand, its antitumor activity was studied with the cancerous PC3 cell line. Here, it can be observed that FcPsomes D outline no anti-tumour activity at any concentration, ensuring its inactivity or biocompatibility at physiological pH in comparison with FcPsomes A and C (Fig. 3(B)). However, when studying GOx-Psomes D in glucose-containing cell media, the simultaneous production of expected hydrogen peroxide and hydroxyl radical during a continuous period provides antitumor activity of GOx-FcPsomes D even at low concentrations (Fig. 3(B)). Results from control experiments with GOx-FcPsomes D in cell media (Fig. S11, ESI†) show that over time the pH does not decrease (Fig. S11, ESI†). This might imply for anti-tumour activity of GOx-FcPsomes D that only the production of radicals in the cell assays is increased, assuming in different (acidic) compartments of PC3 cells and extracellular environment.

The activity of GOx-FcPsomes D was evaluated after three months of storage at −20 °C, using the PC3 cell line (tumor) and the RWPE-1 cell line (non-tumor prostate cells) as models (Fig. 3(C) and (D)), alongside a naked GOx enzyme control with an assumed 10% loading rate (Fig. S15, ESI†). Results demonstrate that the system remains functional after prolonged storage. However, similar levels of toxicity are observed in RWPE-1 cells, underscoring the need for improved specificity or shorter experimental time frames. This issue remains significant when assessing synergistic effects, as the free GOx enzyme exhibits a comparable toxicity profile (Fig. S15, ESI†). One important consideration is the potential overestimation of the GOx concentration, which could impact the observed results. It is well-known that after 24 h of incubation, substantial H_2O_2 accumulation occurs, contributing to a general cytotoxicity of H_2O_2 towards (un)healthy cells. Moreover, EPR studies also demonstrate that these systems generate radicals in a pH-dependent manner. To conclusively confirm the synergistic effect, future investigations should focus on shorter incubation periods and precise quantification of reactive oxygen species (ROS) at the cellular level. A control experiment

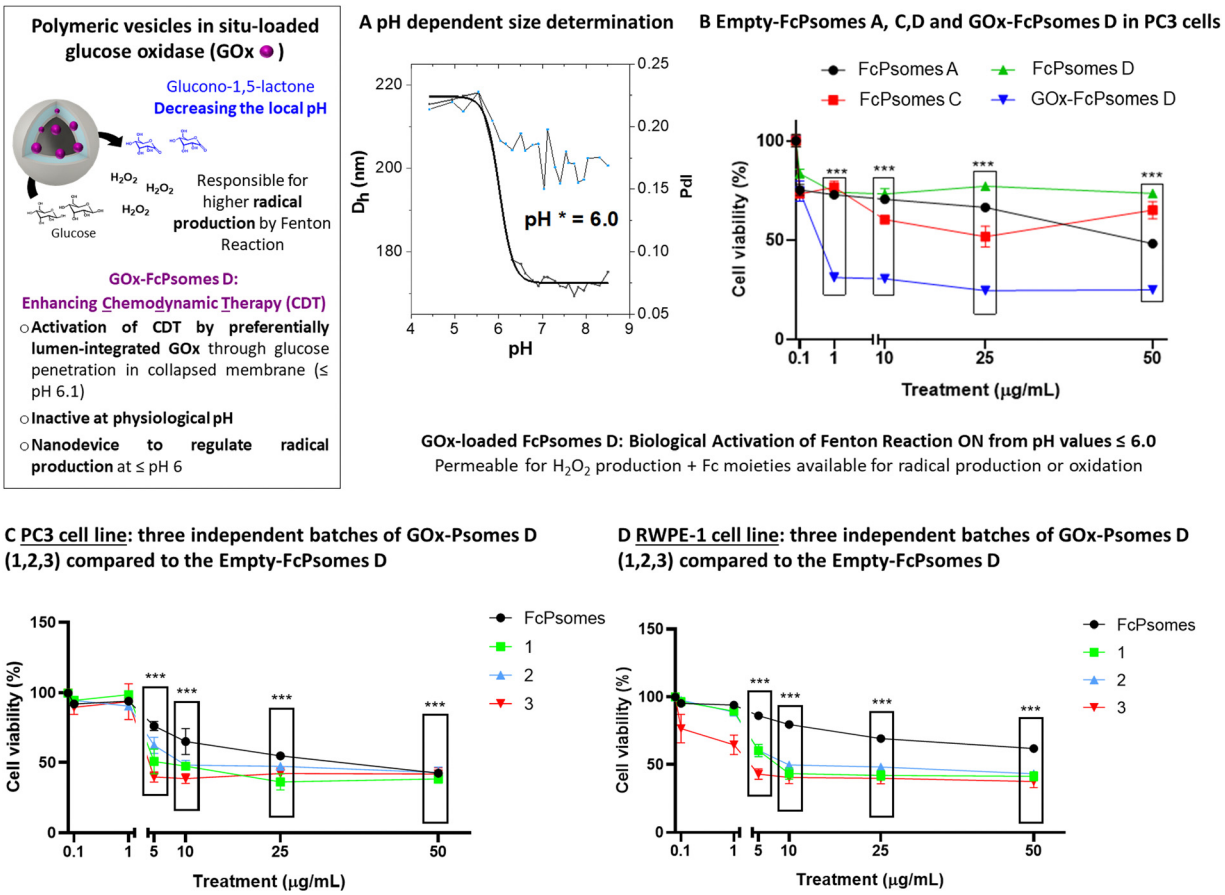

Fig. 3 GOx loaded FcPsomes D allowing biological reactions driven by a spatiotemporal and environmental dependency in a local environment. (A) pH dependent size determination of GOx-loaded FcPsomes D in 1 mM PBS by DLS using 0.5 mg mL^{-1}. The pH* was determined by using Boltzmann fit and taking the inflexion point. (B) Proof of concept of enhancing the ferrocene effect as a producer of radicals by continuous hydrogen peroxide production. Effect of empty-FcPsomes A, C, D and GOx-FcPsomes D at different concentrations on cell viability in the PC-3 cell line (prostate cancer). (C) Enhancement in PC3 cell line using three different batches of GOx-FcPsomes D. (D) Enhancement in RWPE-1 cell line (epithelial cell) using three different batches of GOx-FcPsomes D.

measuring H_2O_2 accumulation in the presence of glucose at the concentrations found in the cell culture medium reveals only a slight reduction with GOx-FcPsomes D (50 μg mL^{-1}) compared to GOx-loaded Psomes D lacking ferrocene units (Fig. S14, ESI†). This result suggests following structure–relationship in GOx-FcPsomes D that H_2O_2, produced, will not be quantitatively destroyed by the tumor-specific activity of most inactive ferrocene units in the collapsed membrane of FcPsomes D at physiological pH as extracted from EPR study (Fig. 2). This also indicates that few GOx are integrated in the outer sphere of FcPsomes D also producing glucono-1,5-lactone besides H_2O_2 in the same concentration range. Due to the buffer capacity of the cell culture glucono-1,5-lactone as proton source is not able to protonate the pH-responsive membrane of FcPsomes D to enhance the activity of ferrocene units at physiological pH. Alternatively, as noted earlier, the system may require a more acidic, tumor-like pH to enhance ferrocene activity. Since the current experiments were performed at physiological pH, future studies under acidic conditions, which more closely mimic the tumor microenvironment, will potentially enhance the exposure and therapeutic efficacy of the ferrocene units, leading to improved antitumor outcomes.

To corroborate once more the potential of the GOx enzyme in the Fc-containing system, FcPsomes D, the breakdown of the interaction between the Fc unit and the Cy-5-labeled beta-cyclodextrin molecule (β-CD-Cy5) was studied. The molecule was incorporated during the preparation process of FcPsomes D and GOx-FcPsomes D. The release process of β-CD-Cy5, monitored by fluorescence spectroscopy (Fig. 4), was studied after 24 h using two concentrations of glucose (1 mM, cytosolic-like conditions; 10 mM, extracellular-like conditions) in the presence of GOx-FcPsomes D. And on the other hand, in the presence of hydrogen peroxide with empty-FcPomes D. It can be observed that after 24 h, the release is independent of the concentration of glucose, since in both cases it is being supplied by continued hydrogen peroxide production of GOx-FcPsomes D. And in the case of direct treatment with hydrogen peroxide for empty-FcPomes D, release is observed in a collapsed state and in a closed state, or it could be assumed, that even in a closed state, release can be promoted at high concentrations of hydrogen peroxide.

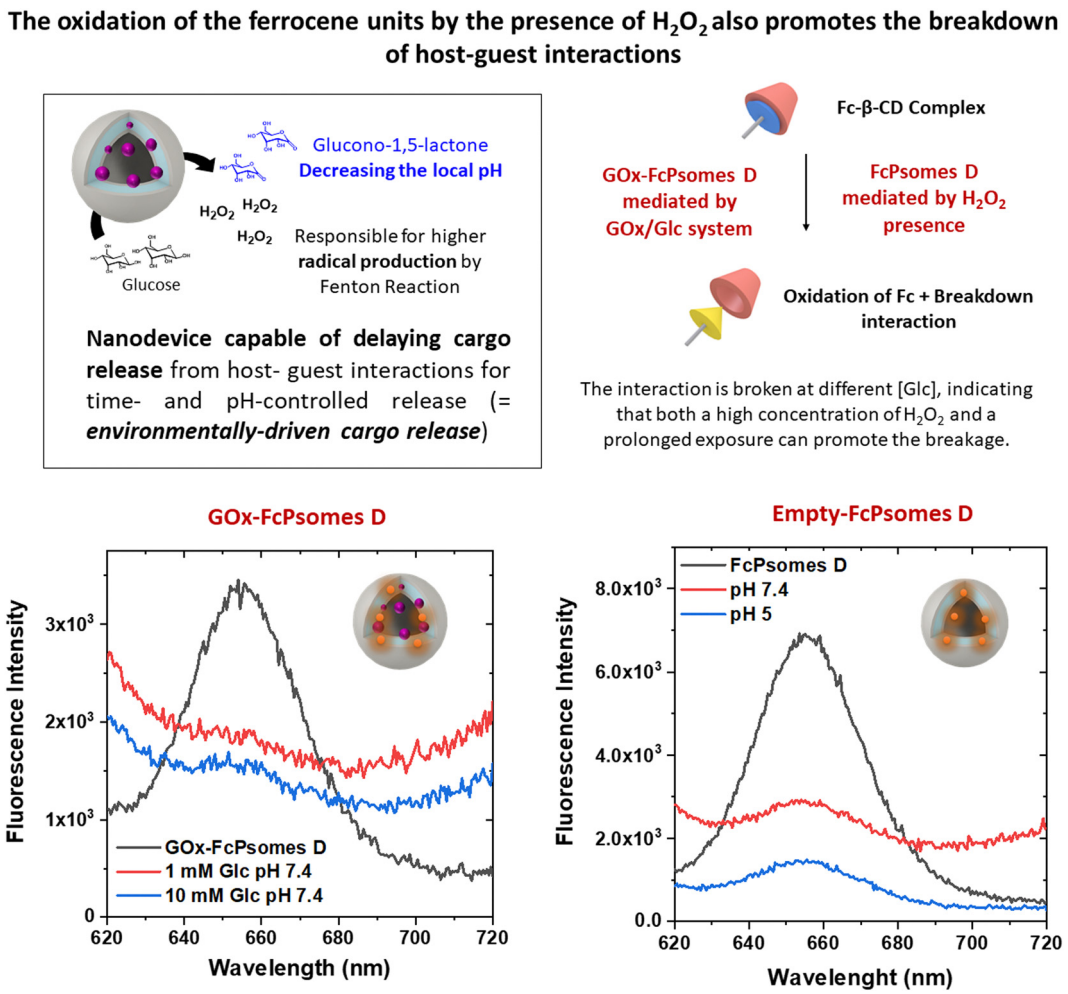

Fig. 4 Proof of concept to enhance the ferrocene effect as a component for redox-responsive host–guest interactions. Oxidation- and pH-dependent release characteristics: combination of pH and oxidation release, proving the combination of host–guest and noncovalent interactions. All samples were studied by fluorescence spectroscopy. β-CD-Cy5 was used. Glucose = Glc.

Experimental

Materials and methods description and additional data are available in the Supporting Information. The methods include synthetic protocols; samples preparation; biological and enzyme assay protocols; characterization procedures.

Conclusions

Today, GOx-containing nanoparticles for CDT, where the enzymatic activity of GOx is used to enhance the production of hydrogen peroxide (H_2O_2) to subsequently participate in Fenton or Fenton-like reactions to produce highly toxic hydroxyl radicals that can induce cancer cell death, represent an important advance in the current search for therapeutic and drug delivery systems.

First, in this study we demonstrate the successful fabrication of ferrocene membrane containing polymeric vesicles (FcPsomes) using improved, controlled and reproducible protocols.[24] The incorporation of GOx within FcPsomes D clearly demonstrates their potential as therapeutic nanoreactors, facilitating a cascade reaction that originates in the vesicle lumen and extends to the outer membrane. This process, driven by the conversion of glucose into H_2O_2 and glucono-1,5-lactone by GOx, activates the ferrocene units, as confirmed by EPR measurements. Additionally, the local generation of gluconic acid may further slightly acidify the microenvironment, favouring the activity of the ferrocene units as radical producers *via* the Fenton reaction, particularly in the swollen state of the FcPsomes D membrane. These dynamic properties allow the membrane to serve as a temporary anchor for biologically active molecules through host–guest interactions.

Our findings indicate that while H_2O_2 is essential to trigger the therapeutic activity of GOx-FcPsomes D, no significant synergistic effects are observed at physiological pH. Moving forward, future studies should focus on directly quantifying ROS production, rather than relying on indirect measurements of H_2O_2, to gain a deeper understanding of the Fenton reaction mechanism. Moreover, developing systems that closely mimic physiological and pathological pH conditions will be critical for

evaluating the selectivity and therapeutic efficacy of ferrocene units in different microenvironments.

In summary, ferrocene-containing polymeric vesicles (FcPsomes) represent a versatile and promising platform for cancer therapy. Their unique ability to integrate controlled drug delivery with redox-triggered release and reactive oxygen species (ROS) generation positions them as a cutting-edge option for improving therapeutic outcomes while minimizing side effects. Beyond cancer therapy, the ability of these vesicles to facilitate cascade reactions may inspire the development of artificial organelles capable of driving complex biological processes, offering potential applications in biomimetics and regenerative medicine.

Author contributions

S. M. carried out experiments, data analyses, project administration, first idea, supervision, writing (first draft), and revision; A. G. V. carried out the majority experiments and data analysis; Y. Z. carried out Cryo-TEM measurements; U. L. carried out experiments and analysed EPR measurements; S. B. carried out AF4 experiments, analysed and interpreted AF4 measurements, manuscript revision; D. A. project administration and manuscript revision.

Data availability

The data supporting this article have been included as part of the ESI.†

Conflicts of interest

There are no conflicts to declare.

Acknowledgements

Mr Andreas Schurig for the synthesis of block copolymers. Ms Alissa Seifert for GPC measurements. Mrs Franzisca Kucharczyk for supporting in crucial control experiments. Chemistry research support centre from University of Alcalá for ICP-OES measurements. Open Access funding enabled and organized by Projekt DEAL. Ondřej Čáp for some preliminary studies. S. M. is supported by the Comunidad de Madrid (Spain) (Programa de Atracción de Talento 2023 *Cesar Nombela*, Ref: 2023-T1/SAL-GL-28977).

References

1 B. Yang, Y. Chen and J. Shi, *Adv. Mater.*, 2019, **31**, 1901778.
2 R. Hu, X. Chen, Z. Li, G. Zhao, L. Ding, L. Chen, C. Dai, Y. Chen and B. Zhang, *Adv. Mater.*, 2023, **35**, 2306469.
3 X. Liu, W. Li, M. Wang, N. Liu, Q. Yang, Y. He, D. Hu, R. Zhu and L. Yin, *Small Methods*, 2023, **7**, 2201641.
4 X. Zhang, H. Guo, X. Zhang, X. Shi, P. Yu, S. Jia, C. Cao, S. Wang and J. Chang, *Biomater. Sci.*, 2023, **11**, 1066–1074.
5 J. Yang, L. Yang, Q. Li and L. Zhang, *J. Colloid Interface Sci.*, 2022, **626**, 719–728.
6 K. Xu, Y. Cui, B. Guan, L. Qin, D. Feng, A. Abuduwayiti, Y. Wu, H. Li, H. Cheng and Z. Li, *Nanoscale*, 2024, **16**, 7786–7824.
7 N. Pn, S. Mehla, A. Begum, H. K. Chaturvedi, R. Ojha, C. Hartinger, M. Plebanski and S. K. Bhargava, *Adv. Healthcare Mater.*, 2023, **12**, 2300768.
8 O. Guliy and L. Dykman, *Biosens. Bioelectron.*, 2024, **19**, 100512.
9 S. Lei, J. Zhang, N. T. Blum, M. Li, D.-Y. Zhang, W. Yin, F. Zhao, J. Lin and P. Huang, *Nat. Commun.*, 2022, **13**, 1298.
10 Y. Na, J. S. Lee, J. Woo, S. Ahn, E. Lee, W. Il Choi and D. Sung, *J. Mater. Chem. B*, 2020, **8**, 1906–1913.
11 Y. Wang, S. Zhang, J. Wang, Q. Zhou, J. F. Mukerabigwi, W. Ke, N. Lu and Z. Ge, *J. Controlled Release*, 2021, **333**, 500–510.
12 R. Cheng, G. Li, L. Fan, J. Jiang and Y. Zhao, *Chem. Commun.*, 2020, **56**, 12246–12249.
13 H. Chen, C. Xing, H. Lei, B. Yan, H. Zhang, T. Tong, Y. Guan, Y. Kang and J. Pang, *J. Controlled Release*, 2024, **368**, 637–649.
14 Q. Zhou, Y. Wang, X. Li, N. Lu and Z. Ge, *Adv. Ther.*, 2021, **4**, 2100130.
15 K. Dong, D. Wang, L. Lin, P. Niu, Y. Wang, Q. Tan and J. Xing, *J. Biotechnol.*, 2024, **383**, 13–26.
16 K. Wang, X. Liu, Y. Jia, L. Pan, M. Shi, W. Pan, N. Li and B. Tang, *Chem. Commun.*, 2024, **60**, 4773–4776.
17 H. Zhang, C. Xing, B. Yan, H. Lei, Y. Guan, S. Zhang, Y. Kang and J. Pang, *Biomacromolecules*, 2024, **25**, 3685–3702.
18 C. Ji, H. Li, L. Zhang, P. Wang, Y. Lv, Z. Sun, J. Tan, Q. Yuan and W. Tan, *Angew. Chem., Int. Ed.*, 2022, **61**, e202200237.
19 J. Tan, H. Li, X. Hu, R. Abdullah, S. Xie, L. Zhang, M. Zhao, Q. Luo, Y. Li, Z. Sun, Q. Yuan and W. Tan, *Chem*, 2019, **5**, 1775–1792.
20 X. Zhang, Y. Ding, Z. Zhang, Y. Ma, X. Sun, L. Wang, Z. Yang and Z.-W. Hu, *Nano Lett.*, 2023, **23**, 7665–7674.
21 C. Cao, X. Wang, N. Yang, X. Song and X. Dong, *Chem. Sci.*, 2022, **13**, 863–889.
22 J. A. Eble and F. F. de Rezende, *Antioxid. Redox Signaling*, 2013, **20**, 1977–1993.
23 X. Wang, S. Moreno, S. Boye, P. Wang, X. Liu, A. Lederer, B. Voit and D. Appelhans, *Adv. Sci.*, 2021, **8**, 2004263.
24 S. Moreno, H. Hübner, C. Effenberg, S. Boye, A. Ramuglia, D. Schmitt, B. Voit, I. M. Weidinger, M. Gallei and D. Appelhans, *Biomacromolecules*, 2022, **23**, 4655–4667.
25 D. Wang, S. Moreno, S. Boye, B. Voit and D. Appelhans, *Macromol. Rapid Commun.*, 2023, **44**, 2200885.
26 H. Gumz, T. H. Lai, B. Voit and D. Appelhans, *Polym. Chem.*, 2017, **8**, 2904–2908.
27 X. Xu, S. Moreno, S. Boye, P. Wang, B. Voit and D. Appelhans, *Adv. Sci.*, 2023, **10**, 2207214.
28 S. Moreno, S. Alex, L. L. Fernandez, U. Lappan, S. Boye, B. Voit and D. Appelhans, *J. Polym. Sci.*, 2023, **61**, 1859–1869.
29 J. Gaitzsch, D. Appelhans, L. Wang, G. Battaglia and B. Voit, *Angew. Chem., Int. Ed.*, 2012, **51**, 4448–4451.

30 X. Wang, S. Moreno, S. Boye, P. Wen, K. Zhang, P. Formanek, A. Lederer, B. Voit and D. Appelhans, *Chem. Mater.*, 2021, **33**, 6692–6700.
31 H. Gumz, S. Boye, B. Iyisan, V. Krönert, P. Formanek, B. Voit, A. Lederer and D. Appelhans, *Adv. Sci.*, 2019, **6**, 1801299.
32 J. Xu, J. Tan, C. Song, G. Zhang, X. Hu and S. Liu, *Angew. Chem., Int. Ed.*, 2023, **62**, e202303829.
33 Z. Jia, J. Zhang, Y. Wei, X. Pan, Z. Hu, R. Kang, X. Zhou and Q. Shen, *Adv. Funct. Mater.*, 2024, **34**, 2309727.
34 Y. Liu, M. Jiang, Z. Zhao, N. Wang, K. Wang and Y. Yuan, *Acta Biomater.*, 2023, **166**, 567–580.
35 H. Oh, E. Jeong, J. S. Lee, J. Kim, D. Lee, B. S. Kim, D. Sung, H. Koo, W. Il Choi and G. Tae, *Mater. Today Bio*, 2023, **22**, 100774.
36 N. Yang, X. Pan, X. Zhou, Z. Liu, J. Yang, J. Zhang, Z. Jia and Q. Shen, *Adv. Healthcare Mater.*, 2024, **13**, 2302752.

